

Advantages of Microwave Sintering in Manufacturing of Anode Support Solid Oxide Fuel Cell

Zhenjun Jiao¹, Naoki Shikazono¹ and Nobuhide Kasagi²

¹ Institute of Industrial Science, the University of Tokyo, 4-6-1 Komaba, Meguro-ku, Tokyo. 153-8505, Japan

² Department of Mechanical Engineering, The University of Tokyo, Bunkyo-ku, Tokyo 113-8656, Japan

Tel.: +81-35452-6777

Fax: +81-35452-6777

zhenjun@iis.u-tokyo.ac.jp

Abstract

Microwave sintering with selective susceptor and spacer has been proved to be an effective and facile method in the manufacturing of anode support solid oxide fuel cell(1). Two anode support SOFCs were fabricated by using microwave sintering and thermal sintering techniques, separately. The performances of the two cells were measured and compared in a temperature range of 700°C to 800°C. The microstructures of the two cells after the measurements were compared qualitatively based on SEM images. FIB-SEM technique was used to reconstruct the 3-D microstructure of both anode and cathode. The quantitative comparison of 3-D reconstructions shows the advantages of using microwave in both anode and cathode sintering processes.

Introduction

As one of the most promising electric power conversion systems, solid oxide fuel cell (SOFC, hereafter) has been identified as an attractive technique in the recent few decades. SOFC working in a high-temperature environment is attracting more attention because of its fuel flexibility, high efficiency and low pollution. In order to achieve long time stability and reducing the equipment cost of the power conversion system, low temperature anode-support SOFC has been investigated by many researchers with an emphasis on reducing the thickness of electrolyte, which dominates the fuel cell resistance. As a result, anode support SOFC attracts more attention because of its high power density with very thin electrolyte(2).

The fabrication of thin film electrolyte onto anode substrate is a challenging procedure in the manufacturing of the whole cell. Zhang et al.(3) reported a novel method for fabricating thin film electrolyte. In their experimental procedures, 10 μm -thick YSZ film was fabricated onto an anode substrate by revolving a rod at low rotation speed. Their cell shows a maximum power density of 1.4 W/cm^2 at 800°C. The anode substrate with thin film electrolyte is sintered at a temperature of 1400°C, and the cathode screen-printed on the electrolyte layer is sintered at a temperature of 1200°C. For most of the researchers, the investigations of SOFC mainly focus on electrode materials and their fabrication processes, and all the cells are sintered by the conventional heating method. Rare papers were published on the new techniques for cell sintering.

Compared to the conventional sintering method which is time-and-energy consuming, some researchers have shown the possibility of using microwave for rapid sintering(4,5). Microwave heating is a self-heating process, which is accomplished by absorbing electromagnetic energy by a dielectric material. Higher heating rate and efficiency can be obtained by using microwave volumetric heating. At room temperature, most of the ceramics have low dielectric loss factor so that it is impossible to raise the temperature. Susceptors made by special material with large dielectric loss coefficient are needed as a pre-heater to raise temperature to the critical value beyond which the material to be sintered can be self-heated(4). In microwave sintering process, the material volumetric heating mechanism makes the sintering process rapid and selective. Fujitsu et al.(4) successfully used microwave energy to achieve the sintering of stabilized zirconia in a 2.45-GHz multimode microwave furnace with selective susceptors. The sintering temperature of zirconia was reduced by 100-150°C comparing to the conventional thermal sintering, and a finer grain size was obtained. In a review of this technique, Clark(6) summarized the fundamentals, benefits, and major research issues of microwave processing of materials.

Microwave heating offers an ultra-fast method for ceramic with an ultra-large heating rate. The grain size uniformity increases because of a few orders higher densification rate in a short sintering time. Only a few groups have investigated the use of microwave sintering in manufacturing SOFC. Oh et al.(7) used GDC as electrolyte and performed microwave sintering for SOFC, which clearly demonstrated the merits of microwave sintering such as lower processing temperature and rapid thermal treatment. The microwave-sintered cell exhibited higher peak power density at 650°C compared to conventional sintered cell with the same materials. In the paper, no systematical work was introduced on the manufacturing procedures and the microstructures comparison between microwave-sintered and thermal-sintered cells. The Only information that was reported is the sintering times, i.e. one hour for anode-electrolyte co-sintering and one hour for cathode sintering.

In this paper, further comparison is conducted between microwave-sintered and conventional-sintered cells on their performances and microstructures.

Experiments

Details of the manufacturing procedures of both microwave-sintered and thermal-sintered SOFCs have already been introduced in our previous paper(1). Mechanically mixed NiO powder and YSZ powder (Semi Co, Japan) were used to prepare NiO-YSZ anode substrate pellets. The powders were mixed at a ratio of 60:40 vol%. In order to maintain a sufficiently porous structure, 10 wt% organic pore former was added to the powder mixture. Microwave susceptor pellets were prepared before the microwave sintering experiments. The microwave susceptor pellets (30 mm in diameter, and 3 mm in thickness) were made by the same technique as substrate pellets, while the material used is $72.5\text{ZnO}-27\text{MnO}_2-0.5\text{Al}_2\text{O}_3$ (ZMA, hereafter). ZMA was prepared by mixing zinc oxide, manganese dioxide and alumina powders (High Purity Chemical Laboratory, Sakado, Japan) (4). YSZ spacer pellets (20 mm in diameter, and 0.8 mm in thickness) were made by YSZ powder (0.3 μm , Tosoh Co, Japan) mixed with 20 wt% ZnO and then sintered in furnace at 1350°C for 2 hours. The spacers were used between the cell and the ZMA susceptor to prevent contamination, and at the same time contributed to the temperature rising up to 1300°C . Pure $\text{La}_{0.8}\text{Sr}_{0.2}\text{MnO}_x$ (LSM) powder (0.4 μm) was used as cathode material in this study. The first group cells with cathode printed were sintered in microwave oven. The second group cells were thermal-sintered.

Cell performance measurement devices

The SOFC performance measurement setup has been introduced in the previous paper(1). Pt meshes was used as current collectors, which were pressed against the electrodes of the cell by mechanical force. Glass rings were used as the seals between two outer alumina tubes, and the two outer tubes were also pressed against the cell by spring. After the temperature was increased beyond 600°C , the glass seals melted and resulted in perfect sealing. The performance of SOFC was evaluated at different temperatures by using humidified hydrogen and pure oxygen. I-V characterization and A-C impedance (frequency range $1-10^6$ Hz) measurements were conducted with a Solatron frequency analyzer (1255B) and a Solatron interface.

Image processing and 3-D reconstruction

Image observation and quantification of the sample microstructures after measurements were facilitated by FIB-SEM (Carl Zeiss, NVision 40). The system is equipped with Gemini FE-SEM column, zeta FIB column and a multi-channel gas injection system (SIINT). 3-D microstructures of both anode and cathode can be virtually reconstructed in a computational field by using 2-D SEM images obtained through the FIB-SEM observation(8,9). Cross-section of the observed sample was first polished by Ar-ion beam cross-section polisher (JEOL Ltd., SM-09010), which results in less damage and smoother cross section compared to the diamond slurry polishing. A layer of carbon was then deposited onto polished surface to indicate the reconstructed region. All the 2-D images were processed in software Matlab for the subsequent reconstruction of 3-D structure in software Avizo (Maxnet Co., Ltd). The comparison between microwave-sintered and thermal-sintered cells was based on the corresponding 3-D reconstruction.

Results and discussions

Fig. 1 shows the comparison of I-V performances between microwave-sintered and conventional thermal-sintered cells. All the measurements were conducted by introducing

H₂ with 3% steam to anode as fuel, and pure oxygen to cathode as oxidant. It is shown that the maximum power densities are 0.12, 0.18 and 0.25 W/cm² for microwave-sintered cell and 0.04, 0.07 and 0.105 W/cm² for thermal-sintered cells at 700°C, 750°C and 800°C, respectively. The Anode-Cathode open circuit potential of microwave-sintered cell is around 0.95 V, which is lower than the theoretical value 1.135 V. The lower open circuit potential indicates the possibility of certain leakage across the thin YSZ film, which is caused by micro-cracks formed in the extremely fast microwave sintering process or measurement heating up process. Besides, the non-uniform electromagnetic field within domestic microwave oven may also lead to the micro-cracks within non-uniform sintering process(1). Without leakage problem, the performance of microwave-sintered cell can be further improved.

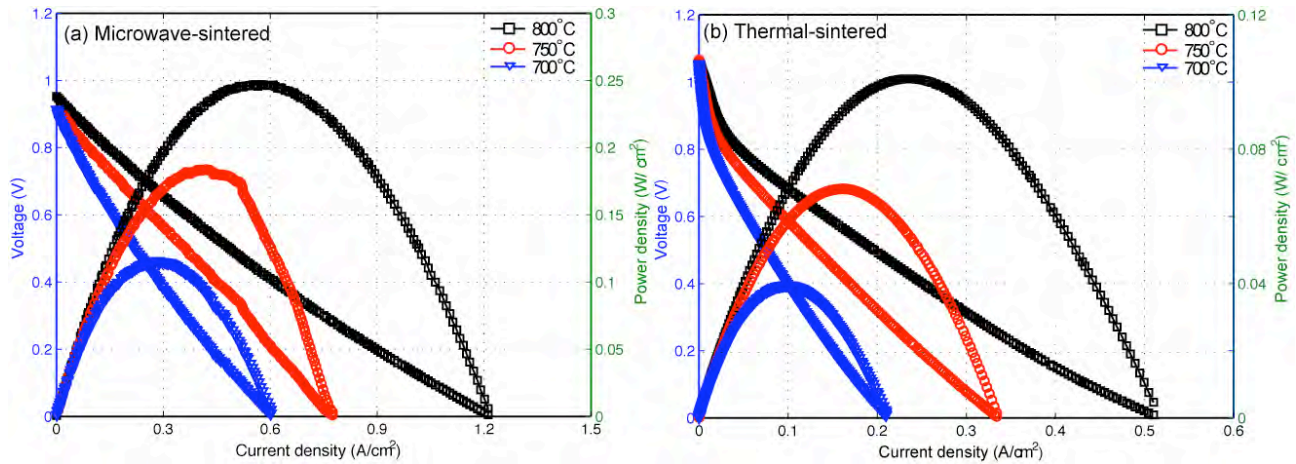


Fig. 1 The I-V characteristics comparison between microwave-sintered and thermal-sintered anode support SOFC at different temperatures. 3% H₂O, 97% H₂ as fuel and 100% O₂ as oxidant.

Fig. 2 shows the comparison of Anode-Cathode impedance spectra between microwave-sintered and conventional thermal-sintered cells. According to the high frequency spectra, the ohmic resistance of the cell sintered by microwave was about 0.55 Ωcm² at 800 °C which is only half of thermal-sintered cell. With the increase of temperature, the ohmic resistance slightly increases in both cases. From 800 °C to 700 °C, for microwave-sintered cell, the electrode polarization increases from 0.5 Ωcm² to 1 Ωcm², while for thermal-sintered cell, the increase is from 5.5 Ωcm² to about 31.5 Ωcm². Both of the impedance changes indicate that low-frequency polarization dominates the cell performance, especially for thermal-sintered cell.

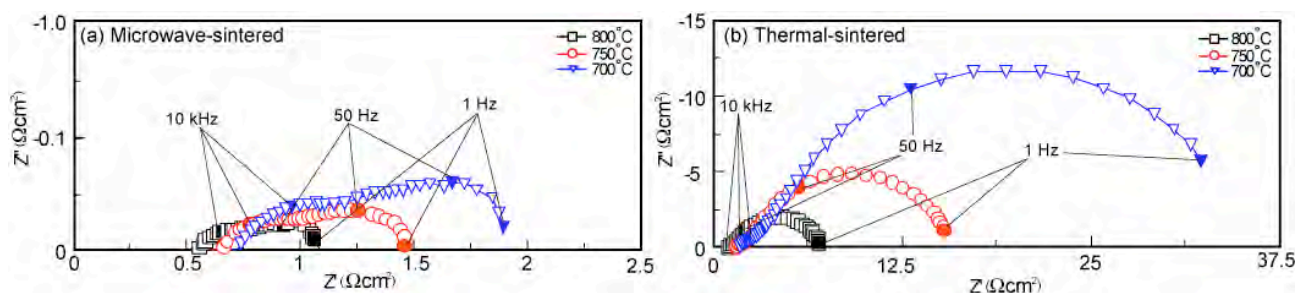


Fig. 2 Anode to cathode impedance spectra comparison between microwave-sintered and thermal-sintered cells.

The microstructures of the cells after testing were examined by SEM. Fig. 3 shows the SEM images of cross-sections, and the top surfaces of anode, electrolyte and cathode for both microwave-sintered and thermal-sintered cells. From the comparison it can be

observed that, with the same materials used, microwave sintering results in very different microstructures from thermal sintering method. Microwave-sintered electrolyte is thinner than that of thermal-sintered one, and both methods resulted in fully densified YSZ film. The thinner electrolyte film in microwave sintering is mainly caused by the mechanical pressing applied by microwave susceptors. After sintering, microwave-sintered cell remained flat while thermal-sintered one was bent. Several microwave-sintered cells were tested, and similar deformations were obtained. For anode, microwave-sintering method produces finer and sharper particles than thermal sintering. For cathode, microwave sintering produced coarser LSM particle than thermal sintering, and the microwave-sintered LSM particle surface is rougher. Certain amount of sub-micron particles was observed uniformly on the particle surface.

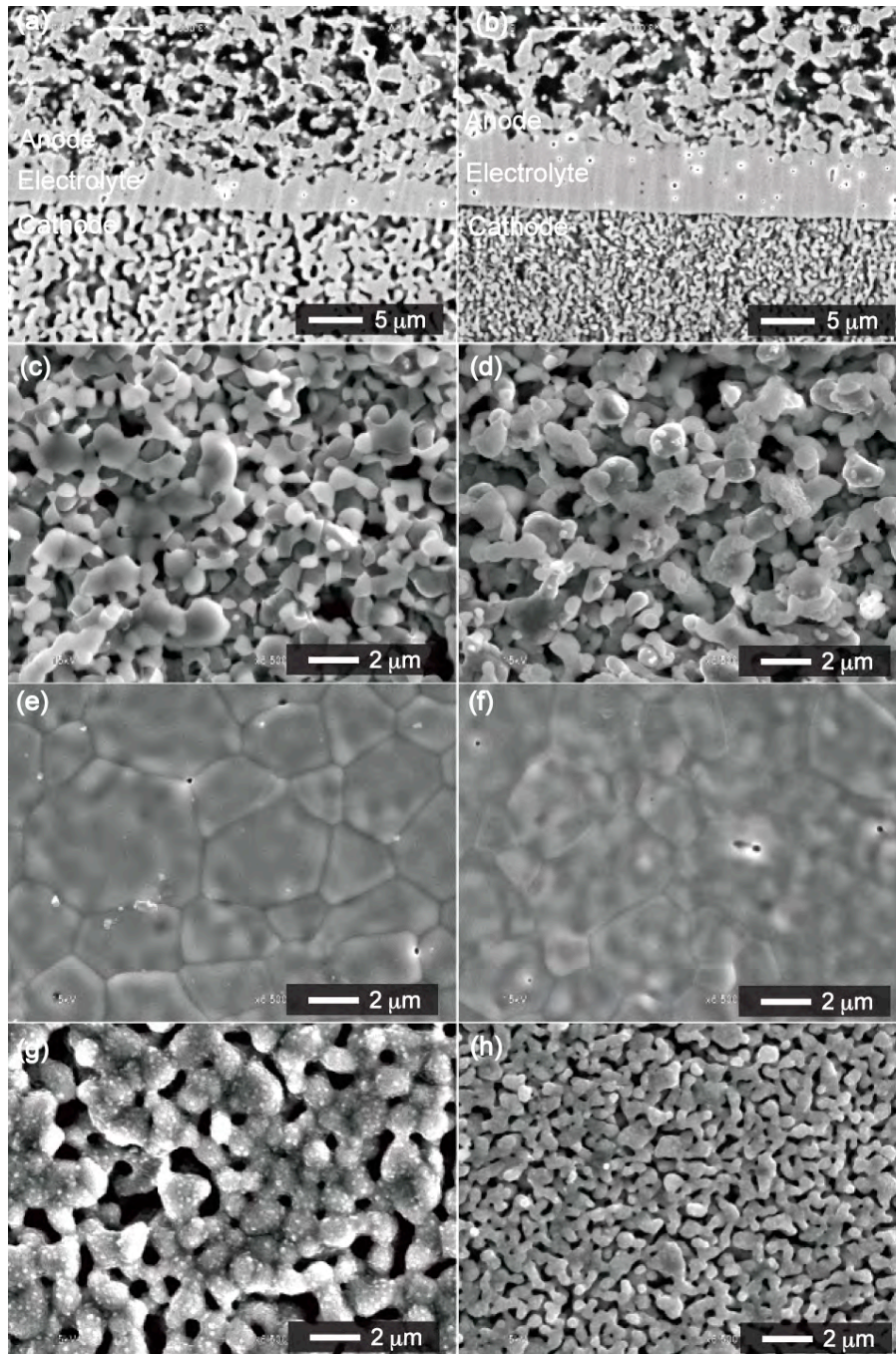


Fig. 3 SEM images of (a) microwave-sintered and (b) thermal-sintered cell cross-section, (c) microwave-sintered and (d) thermal-sintered anode, (e) microwave-sintered and (f) thermal-sintered electrolyte and (g) microwave-sintered and (h) thermal-sintered cathode.

3-D reconstructions

Fig. 4 shows the 3-D reconstruction of the microstructures for both microwave-sintered and thermal-sintered anodes, with separated Ni and YSZ phases. Non-percolated clusters in both Ni and YSZ networks are shown in red color. The connectivities of both Ni and YSZ phase's networks are measured by the volume percentage of the percolated cluster. The microstructural parameters are summarized in Table 1. From the comparison, it can be seen that, with a much shorter sintering time and lower sintering temperature(4), microwave sintering method produces more dense composite anode structure with better phase connections for both Ni and YSZ.

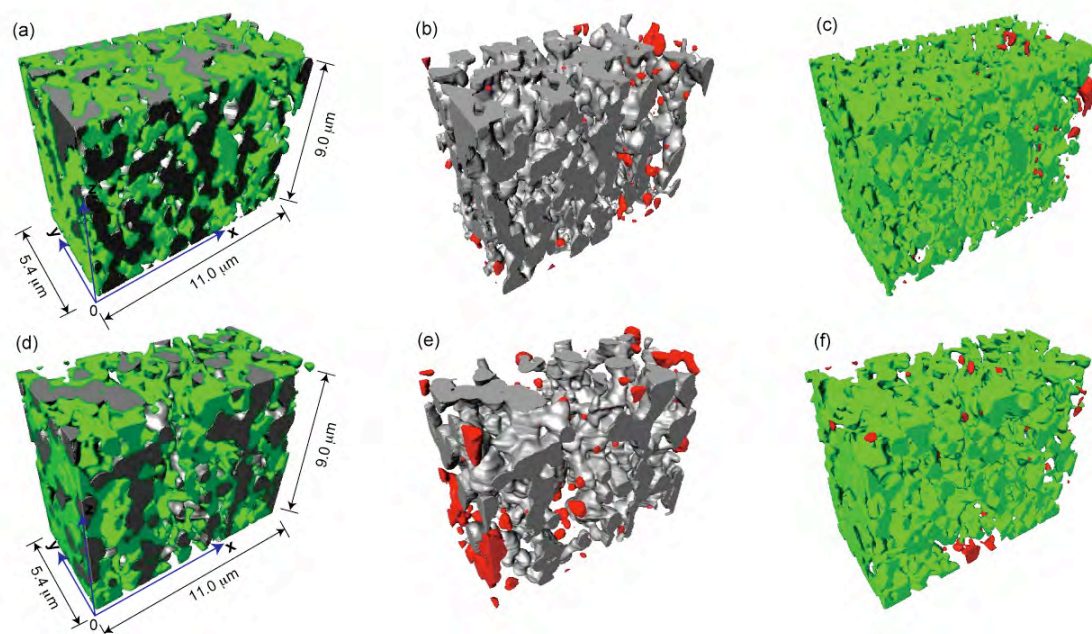


Fig. 4 3-D reconstructions of microwave-sintered (a) composite anode (b) Ni phase and (c) YSZ phase and thermal-sintered (d) composite anode (e) Ni phase and (f) YSZ phase. Red color indicates the non-pocolated particle clusters separated from the main phase network.

Table 1 Energy Microstructural properties comparison between microwave-sintered and thermal-sintered cells based on 3-D reconstruction.

Parameters	Microwave-sintered	Thermal-sintered
Anode Porosity	34.1%	39.7%
Ni percolation percentage	96.2%	93.4%
YSZ percolation percentage	98.9%	98.0%
Cathode Porosity	36.5%	45.0%

In order to further investigate the anode microstructural differences between microwave sintering and thermal sintering methods, TPB densities corresponding to Fig. 4 was calculated. Centroid method was used to calculate the TPB densities(9). TPB density is defined as the length of TPB within unit volume. The total TPB densities and active TPB densities in different directions for both cells are listed in Table 2. It is shown that microwave sintering results in larger total TPB density than thermal sintering, which is due to finer particle size. Only active TPB, which connects current collector to electrolyte, contributes to cell performance. The active TPB densities along three axis directions are nearly the same, which means that both microwave sintering and thermal sintering

produce isotropic anode microstructures. The active TPB density takes possession of 78% of the total density for microwave-sintered anode and 72% for thermal-sintered anode. The higher total TPB density and active TPB density of microwave-sintered anode can partially explain the better performance of microwave-sintered cell.

Table 2 TPB network properties of microwave-sintered and thermal-sintered anodes.

TPB density	Microwave-sintered	Thermal-sintered
Anode	$\mu\text{m}/\mu\text{m}^3$	$\mu\text{m}/\mu\text{m}^3$
Total 3-D TPB density	5.36	4.02
Active TPB density ($x = 0 \rightarrow 11.0 \mu\text{m}$)	4.15	2.89
Active TPB density ($y = 0 \rightarrow 5.4 \mu\text{m}$)	4.15	2.90
Active TPB density ($z = 0 \rightarrow 9.0 \mu\text{m}$)	4.12	2.91
Active TPB density ($x = 11.00 \mu\text{m}$)	4.10	2.93
Active TPB density ($y = 5.4 \rightarrow 0 \mu\text{m}$)	4.15	2.96
Active TPB density ($z = 9.0 \rightarrow 0 \mu\text{m}$)	4.17	2.89
Cathode	$\mu\text{m}/\mu\text{m}^2$	$\mu\text{m}/\mu\text{m}^2$
2-D TPB density	1.7	4.0

Fig. 5 shows the 3-D reconstructions of microwave-sintered and thermal-sintered cathodes. The corresponding porosities for two cathodes are shown in Table 1. It is evident that microwave sintering results in much coarser LSM particle than thermal sintering. This can be explained by the higher sintering temperature and non-thermal driving force which can enhance thermal sintering(6). For pure LSM cathode, TPB concentrates at the interface between cathode and electrolyte and the 2-D TPB densities of two cells are shown in Table 2. It is seen that thermal sintering leads to more than twice TPB density than microwave sintering method, which can not explain the lower impedance of the microwave-sintered cell.

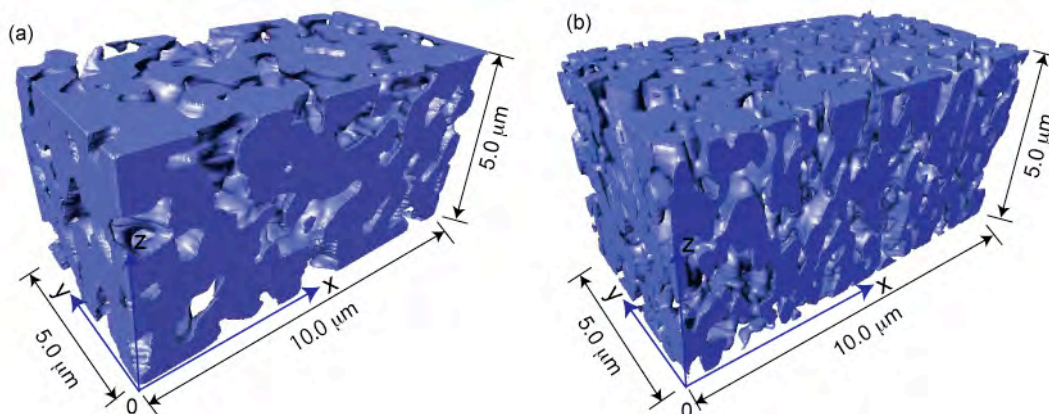


Fig. 5 3-D reconstructions of (a) microwave-sintered cathode and (b) thermal-sintered cathode.

Jiang et al. (10,11) proved that the initial large polarization behavior of freshly prepared LSM cathode is originated from the enrichment of passivation species such as SrO and MnO_x on the LSM particle surface layer. SrO and MnO_x could occupy the active sites and inhibit the surface dissociation and diffusion of oxygen. Cathodic polarization as well as acid etching has been proved to be able to effectively remove or decrease the passivation species from the active sites on LSM surface. The significant improvement of the initial cathode performance caused by the two methods have been proven to reduce the initial cathodic polarization to less than one tenth of the original value, with constant TPB density. Lee et al.(12) investigated the active reaction sites for oxygen reduction in LSM/YSZ electrodes. Surface oxide vacancies as well as the TPB sites are active in oxygen

reduction process. TPB sites are favored since additional diffusional processes are required for the former sites. At lower oxygen pressure, the TPB dominates the surface reaction while the contribution from the surface sites becomes more important at higher oxygen pressure (1 atm). With high oxygen pressure, surface grain boundary diffusion in porous electrode cannot be ignored for its contribution to oxygen reduction, since diffusion in grain boundary is much faster than bulk diffusion. Adler(13) summarized the factors governing oxygen reduction in SOFC cathode. The cathode performance is limited by at least four physical processes: adsorption of oxygen, am-bipolar transport to solid-solid interface, interfacial electrochemical kinetics and ionic transport in the ionic sub-phase, among which TPB density can only dominate the interfacial electrochemical kinetics. With high oxygen pressure, the other three processes may become the rate-determine process and dominate the cathode performance with TPB density. In microwave sintering, the non-thermal effect may result in crystal structure change to the material and influence the final performance of cathode. In our experiments, oxygen inlet pressure was set at 1 atm, which means that grain boundary of LSM also contributed to the cathodic oxygen reduction process, which may even dominate the cathode performance. Even with lower 2-D TPB density at cathode-electrolyte interface, microwave-sintered cathode can show better performance if the concentration of the active surface sites is higher.

In microwave sintering, once the material is heated to a critical temperature via susceptor, the material can be self-heated. Above the critical temperature, the ionic mobility become large enough for the ceramic ions near surface layer to absorb microwave energy and cause dielectric loss due to the ionic movement. Microwave then can interact with ceramic surface through either surface polarization or conduction processes driven by ponderomotive force(14,15). In microwave driving surface polarization process, the high frequency ion oscillation results in microwave-excited ion current, which may result in similar effects as normal electrical current passing through LSM in cathodic polarization. The initial large cathode polarization then can be reduced by microwave driving surface polarization. For the conduction process of mobile ions, ponderomotive force is then defined. Ponderomotive force is defined as a nonlinear force that a charged particle experiences in an inhomogeneous oscillating electromagnetic field(14), which is expressed as,

$$F_p = -\frac{e^2}{4m\omega^2} \Delta E^2$$

where e is the electrical charge of the particle, m is the ion mass, ω is the angular frequency of oscillation of the field, and E is the amplitude of the electric field. This equation shows that a charged particle in an inhomogeneous oscillating field not only oscillates at the frequency but also drifts toward the weak field area. It is known that the sign of the particle charge does not change the direction of the ponderomotive force. Ponderomotive force is thus an electromagnetic force, which is able to move mass. Microwave presents the largest amplitude at ceramic surface and dissipate to zero into the ceramic bulk with a depth of nano-meter scale(15). In the interacting process, all kinds of mobile ions at ceramic surface experience a relatively large ponderomotive driving force towards the ceramic bulk. With this mechanism, continuing crystal vacancies are driven towards the ceramic surface in an opposite direction. The increasing concentration of vacancy may create more active oxygen adsorption sites on LSM surface and then reduce the initial cathodic polarization. At the same time, microwave induced vacancy movement at high temperature may also enhance the thermal sintering process, which leads to much coarser microstructure in a short time sintering time.

In the future, specially designed microwave oven can be used for fabricating anode support SOFC to improve the cell performance. With uniform electromagnetic field and controllable power output, the leakage problem can be solved. For the cell fabricated by thermal sintering, it can also be processed in microwave to improve the cathode performance. The durability comparison between microwave-sintered cell and thermal-sintered cell will be conducted to further investigate the advantages of microwave sintering technique. With ultra-fast heating up process and more outstanding cell performance, microwave sintering can be applied in SOFC fabrication as a new technique with much higher efficiency compared to conventional sintering process.

Summary

Anode support SOFCs were fabricated by both microwave-sintering and thermal sintering methods. The cell performances in the intermediate temperature range of 700-800°C were measured. Microwave-sintered cell shows much better performance than thermal-sintered one. The reconstructed 3-D structures were used to quantify microstructural parameters such as porosity, percolation percentage and TPB density. The higher active TPB densities show the advantages of microwave-sintered anode. The reconstructions of cathode show that microwave sintering results in coarser cathode structure and lower TPB density. Microwave-sintered cathode is proven to have much better performance than thermal-sintered one because of the enhancement of active surface sites for oxygen adsorption.

- [1] Z. Jiao, N. Shikazono, N. Kasagi, *J. Power Sources* 195 (1) (2009) 151.
- [2] S. P. S. Badwal, M. J. Bannister, R. H. J. Hannink, *Science and Technology of Zirconia V*, Technomic publishing Company, 1993.
- [3] Y. Zhang, X. Huang, Z. Lu, Z. Liu, X. Ge, J. X. X. Xin, X. Sha, W. Su, *J. Am. Ceram. Soc.* 89 (2006) 2304.
- [4] S. Fujitsu, M. Ikegami, T. Hayashi, *J. Am. Ceram. Soc.* 8 (2000) 2085.
- [5] M. A. Janney, C. L. Calhoun, H. D. Kimrey, *J. Am. Ceram. Soc.* 2 (1992) 341.
- [6] D. E. Clark, *Annu. Rev. Mater. Sci.* 26 (1996) 299.
- [7] E. O. Oh, H. Kim, D. C. Baek, J. Park, H.-R. Kim, J.-H. Lee, H.-W. Lee, C. M. Whang, J.-W. Son, *ECS Transactions* 7 (2007) 743.
- [8] H. Iwai, N. Shikazono, T. Matsui, H. Teshima, M. Kishimoto, R. Kishida, D. Hayashi, K. Matsuzaki, D. Kanno, M. Saito, H. Muroyama, K. Eguchi, N. Kasagi, H. Yoshida, *J. Power Sources* 195(4) (2010) 955.
- [9] N. Shikazono, D. Kanno, K. Matsuzaki, H. Teshima, S. Sumino, N. Kasagi, *J. Electrochem. Soc.* (2010) in press.
- [10] S. P. Jiang, J. G. Love, J. P. Zhang, M. Hoang, Y. Ramprakash, A. E. Hughes, S. P. S. Badwal, *Solid State Ionics* 121 (1999) 1–10.
- [11] S. P. Jiang, J. G. Love, *Solid State Ionics* 138 (2001) 183–190.
- [12] H. Y. Lee, W. S. Cho, S. M. Oh, H. D. Wiemhofer, W. Gopel, *J. Electrochem. Soc.* 142 (1995) 2659.
- [13] S. B. Adler, *Chem. Rev.* 104 (2004) 4791.
- [14] J. H. Booske, R. F. Cooper, S. A. Freeman, K. I. Rybakov, V. E. Semenov, *Phys. Plasm.* 5 (1998) 1664.
- [15] S. A. Freeman, J. H. Booske, R. F. Cooper, *J. Appl. Phys.* 83 (1998) 5761.